Primitive-Equation-Based Low-Order Models with Seasonal Cycle. Part I: Model Construction

ULRICH ACHATZ

Leibniz-Institut für Atmosphärenphysik an der Universität Rostock, Kuehlungsborn, Germany

J. D. OPSTEEGH

Royal Netherlands Meteorological Institute, De Bilt, Netherlands

(Manuscript received 21 June 2001, in final form 9 July 2002)

ABSTRACT

In a continuation of previous investigations on deterministic reduced atmosphere models with compact state space representation, two main modifications are introduced. First, primitive equation dynamics is used to describe the nonlinear interactions between resolved scales. Second, the seasonal cycle in its main aspects is incorporated. Stability considerations lead to a gridpoint formulation of the basic equations in the dynamical core. A total energy metric consistent with the equations can be derived, provided surface pressure is treated as constant in time. Using this metric, a reduction in the number of degrees of freedom is achieved by a projection onto three-dimensional empirical orthogonal functions (EOFs), each of them encompassing simultaneously all prognostic variables (winds and temperature). The impact of unresolved scales and not explicitly described physical processes is incorporated via an empirical linear parameterization. The basis patterns having been determined from 3 sigma levels from a GCM dataset, it is found that, in spite of the presence of a seasonal cycle, at most 500 are needed for describing 90% of the variance produced by the GCM. If compared to previous low-order models with quasigeostrophic dynamics, the reduced models exhibit at this and lower-order truncations, a considerably enhanced capability to predict GCM tendencies. An analysis of the dynamical impact of the empirical parameterization is given, hinting at an important role in controlling the seasonally dependent storm track dynamics.

1. Introduction

The development of a reduced model of atmospheric dynamics is an attempt at explicitly dealing only with the essential degrees of freedom represented by the climate attractor while still not giving away much realism in comparison to nature or standard general circulation models (GCMs). It provides an interesting practical test of the complexity of the climate attractor. Besides this more fundamental motivation, and a rather distant aim to eventually also use reduced models in climate change studies, the main incentive for their development originates from the hope that they might serve as improved substitutes for traditional low-order models. These have always been important tools scientists have resorted to when the understanding of fundamental dynamical processes was the aim (e.g., Lorenz 1963; Charney and DeVore 1979; Legras and Ghil 1985; Vautard and Legras 1988; Michelangeli et al. 1995; Hannachi 1997). However, they have shared the weakness of either being only in qualitative agreement with nature or focusing on special areas of the globe. It could be interesting to set some of the lessons we have learned from such models on firmer ground by substantially enhancing their realism. This might eventually also facilitate the study of new problems, which have so far been out of reach for low-order modeling.

A few words seem appropriate clarifying our definition of a reduced model. Clearly, this term is already justified if applied to any model using simplifications that go further than traditional spatial filtering, for example, by severe spectral truncation, or dynamical filtering, as, for example, done in quasigeostrophic models. An important class of dynamical simplifications is represented by linear models supplemented by stochastic forcing. They have been quite successful in the description of several aspects of the climate system, be it atmospheric transient eddy activity (e.g., Farrell and Ioannou, 1993, 1994; Whitaker and Sardeshmukh 1998; DelSole and Hou 1999; Zhang and Held 1999) or tropical SST variability (Penland and Matrosova 1994; Penland and Sardeshmukh 1995). It is noteworthy, however, that in some of these studies it was not only the parameterization of the nonlinear impact by linear damping

Corresponding author address: Dr. Ulrich Achatz, Institut für Atmosphärenphysik an der Universität Rostock, Schloßstr. 6, 18225, Kuehlungsborn, Germany.
E-mail: achatz@iap-kborn.de

and additive noise that led to an especially simple description. Additionally, the use of a basis of empirical orthogonal functions (EOFs) also provided a state space compression that goes far beyond the reaches of traditional spectral expansions. This brings us to our personal definition of a reduced model: irrespective of the dynamical equations employed *it should contain a state space description as compact as possible while retaining realism and comprehensiveness.* Given a certain low model dimension, this is to be achieved by 1) the use of optimal basis patterns and 2) suitable parameterizations of the impact of unresolved scales and processes. Furthermore, we want to have a model formulation that can describe in some sense the impact of changes in the large-scale state of the system onto its local linear dynamics and onto the nonlinear fluctuating forcing of the larger scales by the smaller ones. In the context of stochastic modeling, this seems to be a difficult problem, which is just beginning to be mastered (DelSole 2001). Therefore, we focus here on reduced models that are *nonlinear and deterministic*.

In practice the optimal basis is approximated by some near-optimal set. While traditional spherical harmonics are not well suited for this purpose, the aforementioned EOFs provide an appropriate alternative. Several authors have already demonstrated strengths of various atmospheric EOF models (e.g., Rinne and Karhilla 1975; Selten 1995, 1997a,b; Achatz and Branstator 1999, hereafter AB99; d'Andrea and Vautard 2001). Within this context a promising strategy is the use of semiempirical models. These are obtained by projecting an approximate, but still reasonable, dynamical model for the prognostic fields (the dynamical model core) onto the basis patterns and extracting a parameterization of the impact of unresolved scales and not explicitly described processes by empirical means from some reference dataset. A relevant result by AB99 has been that such an EOF model, based on a quasigeostrophic two-layer model core and closed with an empirically determined linear parameterization, is reproducing not only the mean state and transient fluxes but also the leading variance patterns from a perpetual January GCM integration. Nonetheless, both GCM and reduced models did not simulate the seasonal cycle. Furthermore, even for the larger EOF model with 500 basis patterns the local tendency errors were still considerable (about 50%). Finally, the reduced models did not respond correctly to anomalous local heating in the Tropics. The second weakness could possibly be traced back to the use of a quasigeostrophic model core for the global nonlinear dynamics. Even the third problem might, at least in part, be due to this deficiency.

In consequence, this work describes an attempt at extending the realism of semiempirical EOF models by incorporating seasonality and primitive equation dynamics. Section 2 gives an overview of semiempirical reduced models. Section 3 describes our practical implementation: it introduces a primitive equation dynamical model core, describes the determination of global EOFs from some GCM dataset, as well as the extraction of the empirical closure from the same data, analyzes its impact on the predictability of GCM tendencies by our models, and examines how this impact is achieved. Section 4 summarizes and discusses the results. Investigations of the ability of the models to predict the GCM over shorter periods and simulate its climate will be reported in a companion paper, along with an application to weather regimes.

2. Semiempirical reduced models in general

a. Projected model

Reduced models are intended for the compact description of the behavior of complex systems (e.g., a GCM or the atmosphere itself) with a very large number of variables. Concentrating on n variables of prior interest (the *primary state*, typically flow field and temperature at a not-too-fine horizontal resolution and on a limited number of levels), the corresponding state vector $\mathbf{X} \in \Re^n$ is expanded as

$$\mathbf{X}(t) = \mathbf{X}^r + \sum_{\nu=1}^{N} a_\nu(t)\mathbf{e}^\nu + \boldsymbol{\rho}(t), \tag{1}$$

in terms of $N \ll n$ orthonormal basis vectors $\mathbf{e}^\nu$ so that the residual error $\boldsymbol{\rho}$ (comprising all components of the primary state that will not be resolved in the reduced model) is near to its possible absolute minimum, if averaged over all states on the attractor (assuming stationarity). Here, $\mathbf{X}^r$ denotes a reference state. The variables of a reduced model are the expansion coefficients $a_\nu(t)$, which can be obtained from the primary state vector by means of a suitably defined scalar product:

$$a_\nu(t) = (\mathbf{e}^\nu, \mathbf{X}(t) - \mathbf{X}^r). \tag{2}$$

In this work EOFs are used as basis patterns. These can be obtained from a sufficiently large number of observations of the system in a rather straightforward manner: if $\mathbf{S} = \overline{(\mathbf{X} - \mathbf{X}^r)(\mathbf{X} - \mathbf{X}^r)^{\mathrm{T}}}$ (overbars indicate averaging over all data), then the EOFs are solutions of the eigenvalue problem $\mathbf{SM}\mathbf{e}^\nu = \lambda_\nu^2\mathbf{e}^\nu$. Here, $\mathbf{M}$ is the metric defining the scalar product. The residual error in (1) is minimized by picking those N patterns with the largest eigenvalues, that is, variances explained. For the reference state we take $\mathbf{X}^r = \overline{\mathbf{X}}$.

Some considerations are necessary in the specification of the dynamical equations of the reduced model. One must choose some set of functions $r_\nu(\mathbf{a})$ so that solution of $\dot{\mathbf{a}} = \mathbf{r}(\mathbf{a})$ yields a good approximation of the true time dependence of the vector $\mathbf{a}$ of expansion coefficients. As has been shown (Achatz and Schmitz 1997; Selten 1997b; AB99), such a model can be obtained by a strategy consisting of two parts. In the first step one takes approximate tendencies $\mathbf{g}(\mathbf{X}) \approx \dot{\mathbf{X}}$ for the primary state (henceforth called the *dynamical model core*), based on the fundamental geophysical fluid dy-

namical equations, and uses it for calculating the interaction between the resolved components. In the second step, one resorts to empirical means for obtaining a parameterization of the impact of all unresolved components and of all physical processes that are not described by the dynamical core. The dynamical core should be good enough so that, for all states on the attractor, the residue $\dot{\mathbf{X}} - \mathbf{g}(\mathbf{X})$ between the true tendencies and their approximation is small. The true tendencies $\dot{\mathbf{X}}(\mathbf{X}, \mathbf{Y})$ do not depend only on $\mathbf{X}$ but also on all system variables in the subspace supplementary to the primary state space (e.g., small-scale features, moisture, chemical constituents), to be summarized in a vector $\mathbf{Y}$. Therefore, projecting $\dot{\mathbf{X}}$ onto the basis patterns, with the help of (1) and (2), yields for the tendencies of the expansion coefficients

$$\dot{a}_\nu = t_\nu(\mathbf{a}) + \Delta_\nu(\mathbf{a}, \boldsymbol{\rho}, \mathbf{Y}), \tag{3}$$

where the time derivatives of the *projected model* are given by

$$t_\nu(\mathbf{a}) = \left(\mathbf{e}^\nu, \mathbf{g}\left[\mathbf{X}^r + \sum_{\nu=1}^{N} a_\nu(t)\mathbf{e}^\nu\right]\right), \tag{4}$$

and $\Delta_\nu(\mathbf{a}, \boldsymbol{\rho}, \mathbf{Y}) = (\mathbf{e}^\nu, \dot{\mathbf{X}}(\mathbf{X}, \mathbf{Y})) - t_\nu(\mathbf{a})$ represents the impact of the unresolved components, given by $\boldsymbol{\rho}$ and $\mathbf{Y}$.

Obviously, the metric is important, both for the determination of the EOFs, and for the model projection. Our corresponding choice is influenced by two considerations. First of all, it is interesting to note that nonlinear instabilities (Phillips 1959) are not automatically excluded if any metric is chosen for the projection. It might happen that the nonlinear interactions obtained from (4) create energy leading to unbounded growth. Avoidance of this potential pitfall is desirable whenever possible. In fact, it has been shown by AB99 that *if* 1) the dynamical model core conserves total energy, 2) total energy can be written as a quadratic function of the variables—that is, $E = \mathbf{X}^{\mathrm{T}}\mathbf{M}^E\mathbf{X}$—with the total energy metric $\mathbf{M}^E$ being a positive definite symmetric matrix, 3) the nonlinearities in $\mathbf{g}(\mathbf{X})$ are of polynomial form, and 4) the basis patterns are orthonormal with respect to the total energy metric—that is, $\mathbf{e}^{\nu\mathrm{T}}\mathbf{M}^E\mathbf{e}^\mu = \delta_{\nu\mu}$—*then* projection of $\mathbf{g}(\mathbf{X})$ onto the basis patterns using this metric yields nonlinear terms that conserve turbulent energy $\mathbf{a}^{\mathrm{T}}\mathbf{a}$. Furthermore, in the EOF analysis the metric decides which weights are assigned to variables of different physical character, such as temperature and velocities. This was additional motivation for us to pick a total energy metric since this weights each variable in a dynamically plausible way, according to the total energy variance associated with it. Details of the the dynamical core and its total energy metric will be discussed in section 3a.

b. Empirical closure and dissipation tuning

In the second step of the semiempirical approach an attempt is made to express the impact of the unresolved components onto the resolved part as a function of the reduced model variables alone, that is, to derive a function $\delta_\nu(\mathbf{a}, \boldsymbol{\alpha}) \approx \Delta_\nu(\mathbf{a}, \boldsymbol{\rho}, \mathbf{Y})$ where $\boldsymbol{\alpha}$ is a vector of constant closure parameters. The approximate equality should hold in some reasonable average sense. Derivation of such a parameterization from the basic geophysical fluid dynamical equations by purely analytical means is a tremendous task. We resort, therefore, to a more practical approach, that is, specification of a functional form for all δ_ν, and empirical extraction of the closure parameters from a dataset with sufficiently many observations of $\mathbf{X}$ and its tendencies. This is done by minimizing the mean relative error between model tendencies $\dot{a}_\nu = t_\nu(\mathbf{a}) + \delta_\nu(\mathbf{a}, \boldsymbol{\alpha})$ and their observed counterparts $(\mathbf{e}^\nu, \dot{\mathbf{X}})$:

$$\epsilon_t = \frac{\overline{\sum_{\nu=1}^{N} [(\mathbf{e}^\nu, \dot{\mathbf{X}}) - t_\nu(\mathbf{a}) - \delta_\nu(\mathbf{a}, \boldsymbol{\alpha})]^2}}{\overline{\sum_{\nu=1}^{N} (\mathbf{e}^\nu, \dot{\mathbf{X}})^2}}. \tag{5}$$

It is understood that for each observation $\mathbf{a}$ is calculated from $\mathbf{X}$ by use of (2). In the present work we have used

$$\boldsymbol{\delta}(\mathbf{a}, \boldsymbol{\alpha}) = \mathbf{F}(t) + \mathbf{L}(t)\mathbf{a}; \tag{6}$$

$$\mathbf{F}(t) = \mathbf{F}_0 + \sum_{n=1}^{2} [\mathbf{F}_n^c \cos(n\Omega t) + \mathbf{F}_n^s \sin(n\Omega t)]; \tag{7}$$

$$\mathbf{L}(t) = \mathbf{L}_0 + \sum_{n=1}^{2} [\mathbf{L}_n^c \cos(n\Omega t) + \mathbf{L}_n^s \sin(n\Omega t)]. \tag{8}$$

Here, Ω is the angular frequency of the earth's circumsolar orbit. The parameter vector to be adjusted in the tendency error minimization contains the coefficients of $\mathbf{F}_0$, $\mathbf{F}_n^{c,s}(n = 1, 2)$, $\mathbf{L}_0$, and $\mathbf{L}_n^{c,s}(n = 1, 2)$. In an initial attempt, we had also tried a parameterization with time-independent linear operator $\mathbf{L}$. The resulting model failed, however, in producing a seasonal dependence of the transient fluxes.

Experience has shown that empirical determination of the closure parameters by the above-described method is sufficient if the reduced model equations can predict the true tendencies very accurately (Achatz and Schmitz 1997). However, if the relative tendency error after minimization is still not negligible, typically the model's dissipation is not tuned well yet so that it tends to be too energetic when integrated. Some a posteriori tuning of a suitably defined, in general very weak, damping must therefore be performed in addition. Here this has been done by adding to the tendency of each EOF an additional newtonian damping $-h_\nu[a_\nu - a_\nu^s(t)]$ with

$$h_\nu = A\left(\frac{\nu}{N}\right)^\beta. \tag{9}$$

Here, $a_\nu^s(t)$ is the climate mean in its seasonal dependence, represented, just as the closure terms, by a con-

TABLE 1. Newtonian damping parameters used for the semiempirical models.

Number of EOFs	A (day^{-1})	β
10	8.9×10^{-2}	1.2
20	2.5×10^{-2}	1.6
30	2.6×10^{-2}	1.7
40	2.6×10^{-2}	1.9
50	2.1×10^{-2}	1.9
60	2.6×10^{-2}	1.4
100	6.6×10^{-2}	2.5
200	1.1×10^{-1}	2.1
500	3.0×10^{-1}	1.3

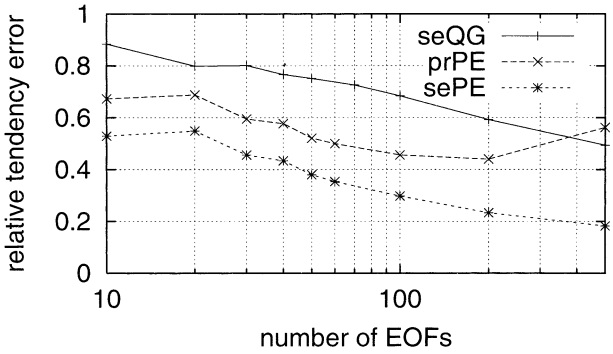

FIG. 1. The relative error in the prediction of GCM tendencies (in a dataset with seasonal cycle) by the semiempirical (se PE) and projected reduced (pr PE) models with primitive equation core, depending on the number of EOFs the model is based on. Also shown are the corresponding results from AB99 for the prediction of tendencies in a perpetual-January dataset of a GCM by a semiempirical reduced (se QG) model with a quasigeostrophic two-layer model core.

stant part, an annual component, and a semiannual component—all of them estimated from the reference dataset. The constants A and β have been determined for each semiempirical model by minimizing the *relative climate error*

$$\epsilon_c = \frac{1}{24} \sum_{m=1}^{12} (\epsilon_1^m + \epsilon_2^m), \tag{10}$$

which is an average quantity calculated from the seasonally dependent relative error of the first moments

$$\epsilon_1^m = \frac{\sum_{\nu=1}^{N} (\overline{a}_{\nu\,\text{model}}^{\,m} - \overline{a}_{\nu\,\text{data}}^{\,m})^2}{\sum_{\nu=1}^{N} (\overline{a}_{\nu\,\text{data}}^{\,m})^2}, \tag{11}$$

and the corresponding second-moment error

$$\epsilon_2^m = \frac{\sum_{\nu=1}^{N}\sum_{\mu=\nu}^{N} (\overline{a'_\nu a'_\mu}^{\,m}_{\text{model}} - \overline{a'_\nu a'_\mu}^{\,m}_{\text{data}})^2}{\sum_{\nu=1}^{N}\sum_{\mu=\nu}^{N} (\overline{a'_\nu a'_\mu}^{\,m}_{\text{data}})^2}. \tag{12}$$

The upper index m, running from 1 to 12, indicates the month for which the mean has been calculated; $a'_\nu(t) = a_\nu(t) - \overline{a}_\nu^{\,m}$ denotes transients. Thus, finally summarizing all ingredients, the equations of our semiempirical models become

$$\dot{a}_\nu = t_\nu(\mathbf{a}) + \delta_\nu(\mathbf{a}, \boldsymbol{\alpha}) - h_\nu[a_\nu - a_\nu^s(t)]. \tag{13}$$

3. Primitive equation semiempirical reduced models

a. The dynamical model core and its total energy metric

As seen above we demand the dynamical core to be energy conserving in its discretized form, the conserved total energy should be a quadratic function of the prognostic variables, and the nonlinearities of the model should be of polynomial form. Owing to the energy conservation requirement we have decided to use a longitude–latitude gridpoint model along the ideas of Arakawa and Lamb (1977, 1981) and Takano and Wurtele (1982). Unfortunately, total energy in the standard primitive equation system is not a positive definite quadratic function of the prognostic variables. In order to circumvent this problem we have reformulated and filtered the equations so that potential temperature is replaced as prognostic variable by its square root $\tau = \sqrt{\theta}$, and surface pressure is left time independent. As to the former replacement, care must be taken to ensure that a numerical code using τ as temperature variable still conserves energy. Neglecting the time dependence of surface pressure is more fundamental since it eliminates the external Kelvin waves. This is a standard approach in oceanography (Bryan 1969) where it is known as rigid-lid approximation. In the atmospheric context it has been used for pressure coordinate models by Smagorinsky (1963) and Held and Suarez (1978). The consequence of this filter is nondivergence of the barotropic horizontal flow component $\langle \mathbf{V} \rangle = \int_0^1 d\sigma \mathbf{V}$, i.e. $\boldsymbol{\nabla} \cdot p^s \langle \mathbf{V} \rangle = 0$, following from vertical integration of the continuity equation. Here, p^s denotes surface pressure and $\sigma = p/p^s$. Consequently, there is a barotropic streamfunction Ψ so that $p^s \langle \mathbf{V} \rangle = \mathbf{k} \times \boldsymbol{\nabla} \Psi$, where $\mathbf{k}$ is the vertical unit vector. The prognostic variables of the filtered model are therefore provided by Ψ, the baroclinic flow field $\hat{\mathbf{V}} = \mathbf{V} - \langle \mathbf{V} \rangle$, and τ. Within this framework total energy can be written as

$$E_f = \frac{1}{g} \oint_A dA \frac{|\boldsymbol{\nabla} \Psi|^2}{2p^s} + \frac{1}{g} \oint_V dV p^s \left(\frac{|\hat{\mathbf{V}}|^2}{2} + c_p P \tau^2 \right), \tag{14}$$

with $\oint_A dA = a^2 \int_0^{2\pi} d\lambda \int_{-\pi/2}^{\pi/2} d\phi \cos\phi$, $\oint_V dV = a^2 \int_0^1 d\sigma \int_0^{2\pi} d\lambda \int_{-\pi/2}^{\pi/2} d\phi \cos\phi$, $P = (p/p_0)^{R/c_p}$, and standard notation otherwise. Therefore, here $\mathbf{X}$ shall be the state vector describing the discretization of Ψ, $\hat{\mathbf{V}}$, and τ on a staggered C grid in the horizontal (Arakawa and Lamb

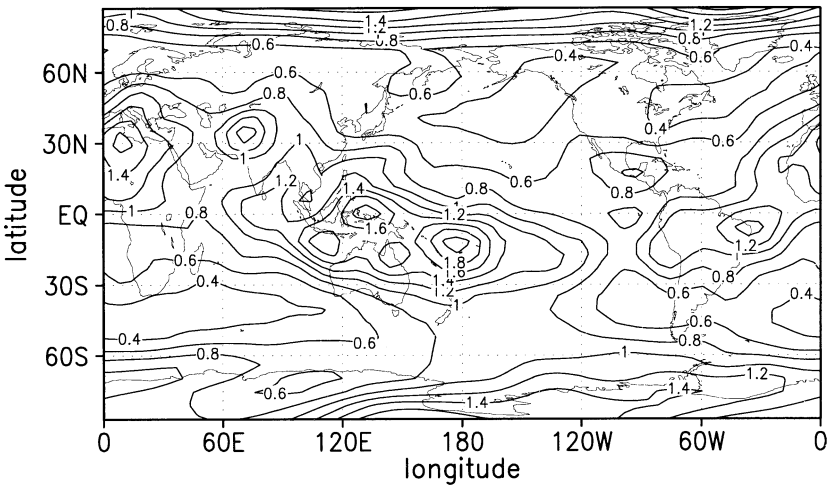

FIG. 2. Spatial distribution of the relative (barotropic streamfunction) tendency error for the projected 500-EOF model. For the comparison, both the predicted and the data tendencies (projected onto the leading 500 EOFs) have been tranformed from EOF representation into grid space, where the comparison has been done pointwise. One hundred years of data have been taken for the analysis.

1977) and σ layers in the vertical. Dynamical core and total energy metric are summarized in the appendix. As for the resolution, we have decided to take three σ layers (at $\sigma = 0.833$, 0.5, and 0.167) and use 64 longitudes and 32 latitudes in the horizontal. The constant surface pressure we have employed is a long time mean from the same data as analyzed below. In extensive tests it has been verified that the filtering does not significantly affect the model dynamics: a benchmark test according to Held and Suarez (1994) was successful. Furthermore, we have introduced as orographically conditioned surface pressure its long time mean from a coupled atmosphere–ocean GCM and compared the model's behavior under solsticial zonally symmetric heating to that of a standard primitive equation code with external Kelvin waves and explicit orography. All mean states and transient fluxes turned out to be virtually the same.

b. The GCM data analysis for global EOFs

The EOFs have been determined from data consisting of half-daily values for horizontal winds, temperature, and surface pressure from a 2000-yr integration of the atmosphere–ocean general circulation model ECHAM3/Large-Scale Geostrophic Ocean GCM (ECHAM3/LSG; Voss et al. 1998). These have been prepared by a linear interpolation from the model's 19 hybrid vertical levels to the three σ layers and a consecutive bilinear interpolation to the staggered horizontal grid. The daily cycle has been removed by averaging between two consecutive states each. With the chosen resolution the matrix to be diagonalized is extremely large ($16\ 256^2$ elements). We have therefore resorted to an iterative approximate determination of the leading variance patterns, relying on successive data compression in orthogonal subspaces with nonglobal EOFs. One hundred years of data were found to be statistically sufficient for an identification of the subspace spanned by the leading EOFs. Inspection of the time series of the corresponding principal components showed that the two leading EOFs are dominated by the strong seasonal cycle, which explains about 30% of the total variance. Nearly 500 EOFs are needed for explaining 90% of the variance on top of the seasonal cycle.

c. Estimation and analysis of the closure

The amount of data used for the tendency minimization (1140 yr) was chosen large enough that a further significant increase does not change the model properties any more, with respect to both short-term prediction and climate simulation. The additional Newtonian damping was determined as described above. For the calculation of the climate error in (10) the models have been integrated over periods of 100 yr. The integration uses a semi-implicit time step in which the seasonally independent linear dynamics are treated implicitly, and the rest by an explicit leapfrog with time filter (Asselin 1972). The optimization of the constants A and β in (9) has been done with the help of a nonlinear simplex optimizer. The resulting parameters are summarized in Table 1. The relaxation time of the first EOF is sufficiently small to ensure that, with the possible exception of the 10-EOF model, a correct reproduction of the seasonal cycle cannot be attributed to this extra term. Furthermore, it also does not affect the following analysis of the impact of the empirical parameterization on the model.

To begin with, solution of the linear regression problem yields tendency error minima for different numbers

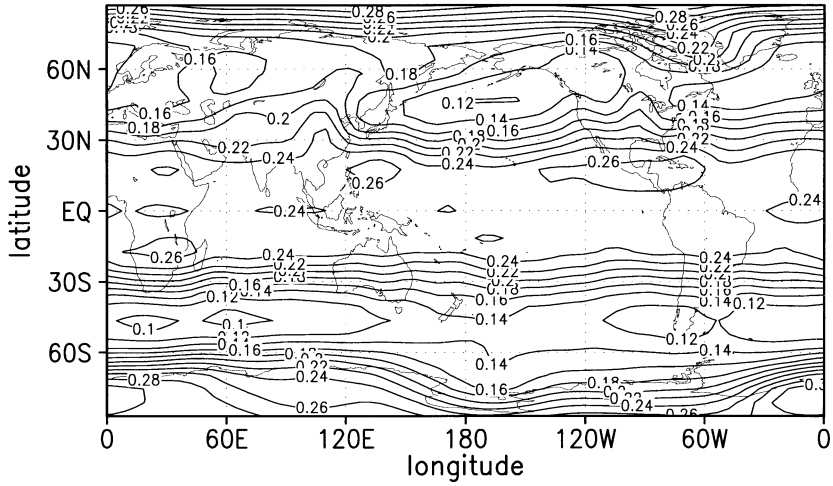

FIG. 3. As in Fig. 2, but for the complete semiempirical model (i.e., with empirical forcing and empirical linear corrections).

of basic EOFs as shown in Fig. 1. The corresponding errors for the projected models, and the relative errors determined by AB99 are also shown. Interestingly, already the projected three-layer primitive equation model performs better than the semiempirical quasigeostrophic two-layer model. The parameterization scheme reduces the errors further by a considerable amount so that we encounter tendency errors of less than 20% for the 500-EOF model. Figure 2 shows the geographical dependence of the error in predicting tendencies of the barotropic streamfunction by the projected 500-EOF model. Whereas this model performs quite well in the storm track regions, there is a conspicuous failure in the Tropics and at the North Pole. As shown in Fig. 3, the empirical closure reduces the overall tendency errors so much that they are smaller than 30% in the Tropics, and near 10% in midlatitudes. Actually it is the linear closure terms that are of decisive importance for a good tendency prediction: the total mean relative tendency error for all prognostic variables is 0.56 for the projected reduced model, 0.48 for the projected model with empirical forcing, and 0.18 for the complete semiempirical model.

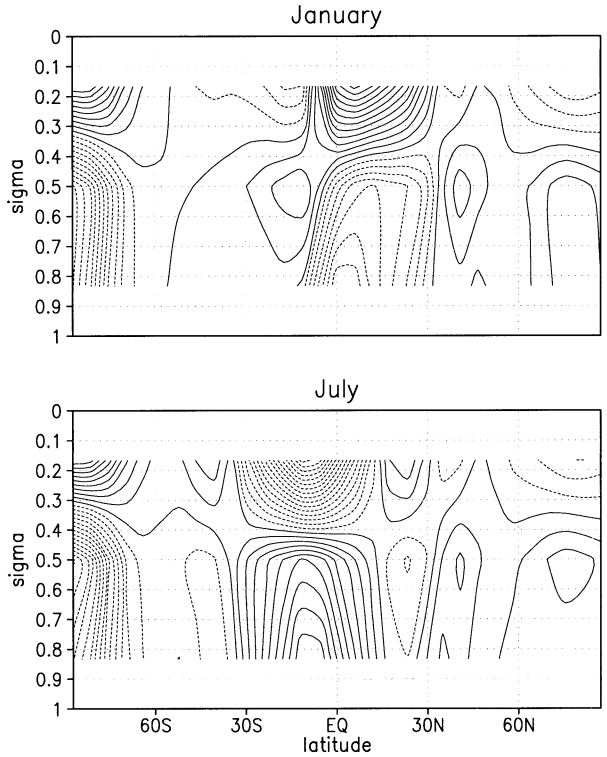

FIG. 4. Zonal mean of the empirical meridional wind forcing in the semiempirical 500-EOF model in Jan and Jul. Contour intervals are 0.05 m s^{-1} day^{-1}. Negative values are dashed.

As for some dynamical features of the 500-EOF closure, Fig. 4 shows the zonal-mean empirical forcing of the meridional wind in January and July. Clearly, there is a tendency to enforce the winter-hemispheric Hadley circulation. Here, one should recall that direct physical forcing components (heating due to radiation, convection, latent heat release, etc.) appear only in the thermodynamic equation. So the fact that fixed empirical forcing terms appear in our momentum equations points at indirect forcing effects that may be understood as the net effect on the resolved components of nonlinear interactions among the unresolved components. That our empirical approach can also yield forcing characteristics one would expect from direct physical parameterizations can be seen in Fig. 5, where the empirical forcing for the lower-level thermodynamic variable is shown. Obviously there is the typical heating pattern for lower-level air masses over land in the summer hemisphere, and the opposite pattern in the winter hemisphere.

Finally, in an attempt to shed some further light on the role of the empirical linear terms, we have linearized

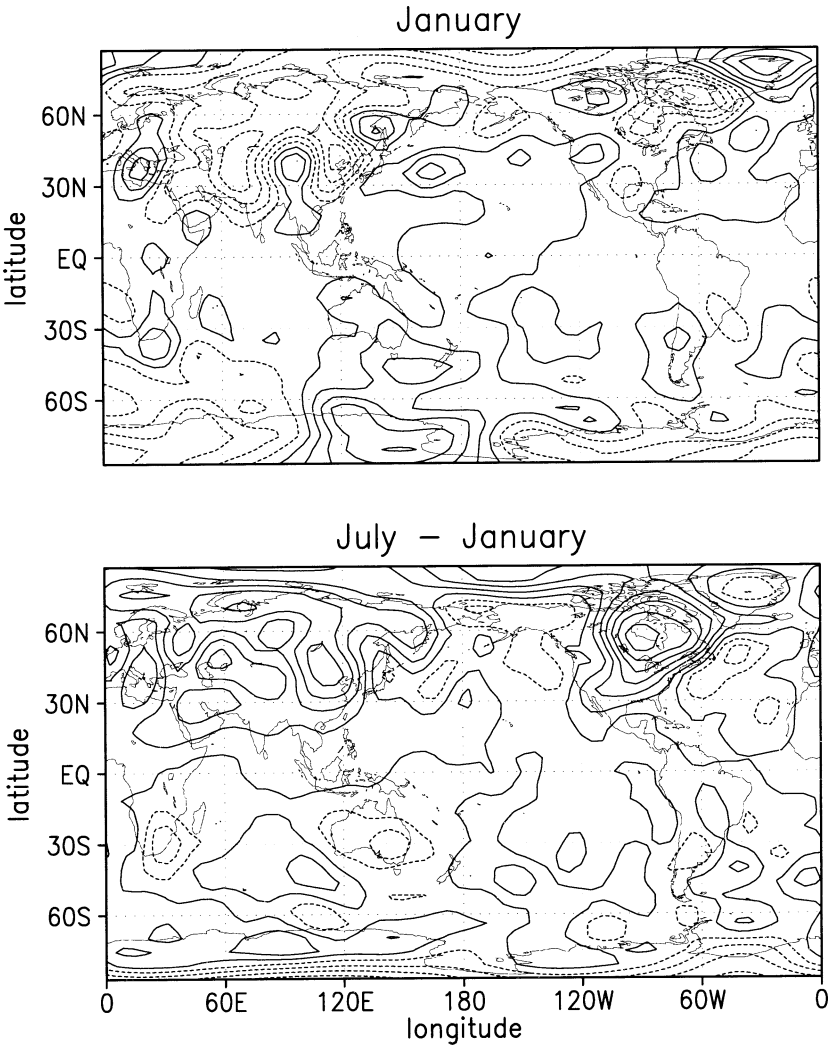

FIG. 5. Jan empirical forcing of the thermodynamic variable τ at $\sigma = 0.833$ in (top) the semiempirical 500-EOF model, and (bottom) the difference between this and the corresponding field in Jul. Contour intervals are 0.02 $\sqrt{\text{K}}$ day^{-1}. Negative values are dashed.

our model, with and without these terms, about the January or July mean state of the GCM. Following the standard procedure (e.g., Farrell and Ioannou 1996) we have then calculated from the thus obtained linear tensor, the leading optimal vectors for 5-day lead time. What ought to be expected as result for a satisfactory model is a storm track mode on the respective winter hemisphere. Indeed, in both months, the leading optimal vector of the semiempirical model is a Pacific storm track mode (Fig. 6), and the following pattern reproduces it with a phase shift (not shown). Patterns 3 and 4 are corresponding Northern-Hemispheric Atlantic storm track modes for January, and further Southern-Hemispheric Pacific storm track modes for July (also not shown). For comparison, Fig. 7 shows the leading optimal vectors from calculations without empirical linear correction. They are quite different from those in Fig. 6, both in scale, spatial extension, and their location on the globe. This shows that the empirical linear terms are actually controlling the seasonally dependent storm track dynamics.

4. Summary and discussion

Our study represents a continuation of previous work on semiempirical reduced models for the atmosphere. Generally, the development of such models is done in two main steps. In the first of those a near-optimal basis of EOFs is projected onto a dynamical model based on the fundamental geophysical fluid dynamical equations (the dynamical core). In the second step the impacts of neglected scales and physical processes are parameterized by an empirical scheme, which is extracted from some dataset by minimization of the difference between observed tendencies and the corresponding prediction of the reduced model. Here the dynamical model core

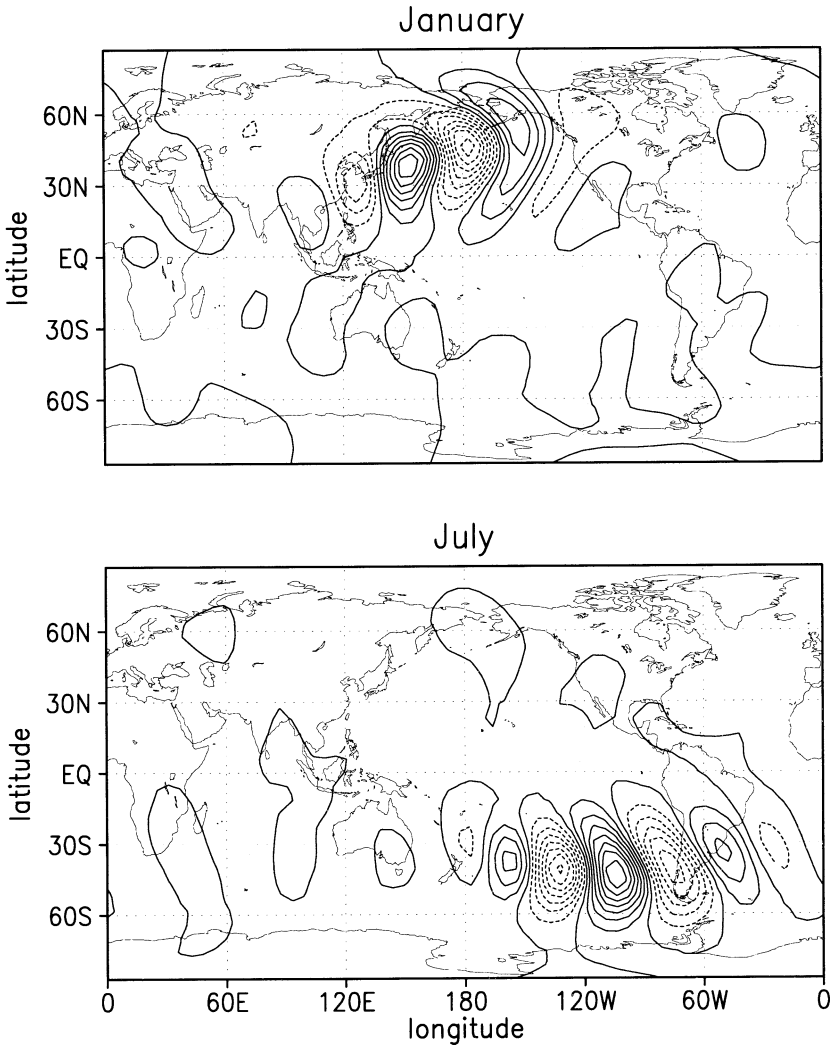

FIG. 6. (top) Barotropic streamfunction signature of the Jan and (bottom) Jul leading optimal vector for 5-day lead time, obtained by linearizing the semiempirical 500-EOF model about the respective monthly mean state of the GCM. The corresponding growth factors are 6.98 in Jan and 6.21 in Jul. Contour intervals are equidistant in meaningless units. Negative values are dashed.

is a primitive equation model that differs from its traditional counterparts by filtering external Kelvin waves. This enables the construction of a total energy metric consistent with the model, which has two main advantages: first, an EOF basis determined from the data with the help of this metric ensures that the projected model has no nonlinear instabilities; second, a natural solution is provided to the question of how to weight in the analysis prognostic variables of different dynamical character (e.g., winds and temperature) with respect to each other. Technically, the filtering of external Kelvin waves is achieved by the use of a time-independent surface pressure, an approach that is parallel to the rigid-lid approximation used in oceanography.

Consequently, our basis patterns are global EOFs describing simultaneously winds and temperature in all three spatial dimensions. They have been determined from atmospheric data of a 2000-yr-long run of a coupled ocean–atmosphere GCM. It is found that, in spite of the presence of the seasonal cycle, the number of patterns necessary for explaining 90% of the variance on top of the seasonal cycle is about 500. This number is in interesting agreement with a previous result (AB 99) from an analysis of streamfunction data in two levels from a perpetual-January GCM dataset. It seems as if the atmosphere is not using different degrees of freedom for different seasons. Seasonality seems more to be brought about by a rearrangement of the respective relevance of the various circulation structures involved. This looks parallel to the findings of Corti et al. (1999)

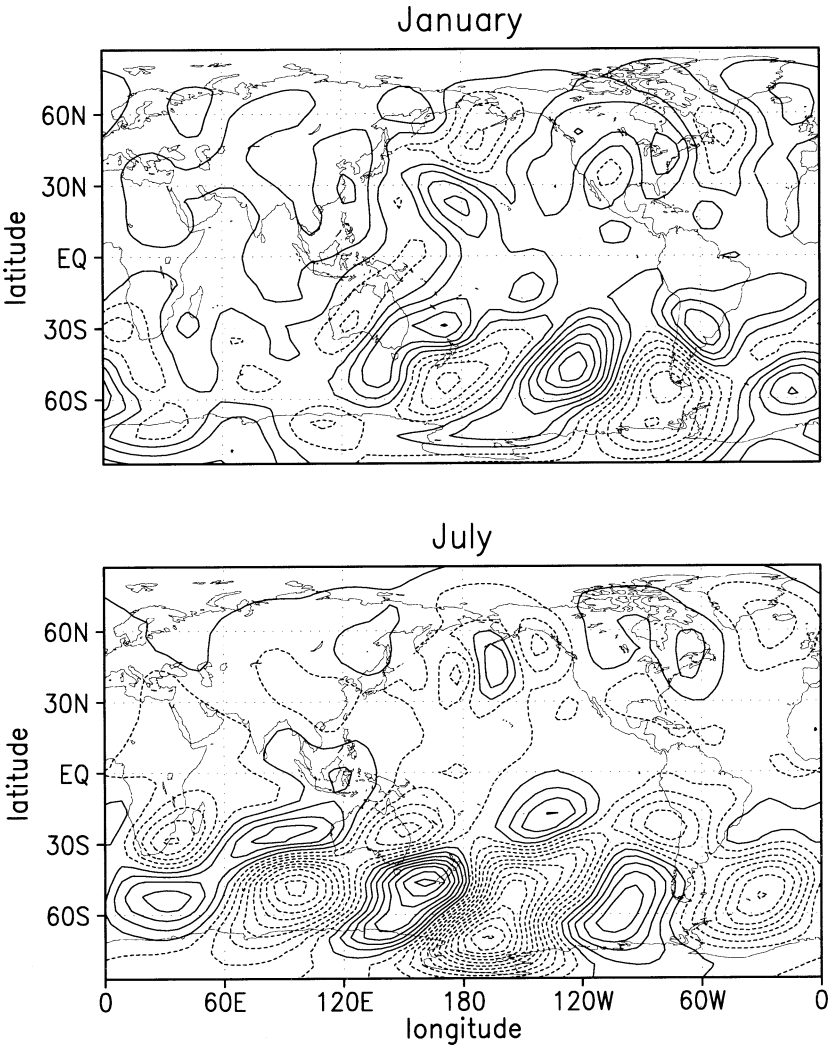

FIG. 7. As in Fig. 6, but for the 500-EOF model without empirical linear correction. The Jan growth factor is 9.46; that for Jul is 9.45.

on the mechanisms of climate change, encouraging us in our hope that EOF models might eventually be also useful for studies of climate variability.

Our empirical closure is of at most first order in the EOF expansion coefficients. The empirical linear operator has as well a seasonal cycle as the zero-order terms, the external forcing. As was to be expected, the primitive equation model core enables the reduced semiempirical models to predict instantaneous tendencies much better than previously used filtered equations. Nonetheless, plenty of room is still left for further improvements by nonlinear physically based parameterization schemes. The incorporation of moisture and explicit radiation might be interesting, as well as modern reduction techniques as, for example, described by Moise and Temam (2000). Finally, higher vertical resolution of the dynamical core could also be important.

An investigation of the empirical forcing fields showed some expected direct effects such as enhanced summertime heating and wintertime cooling of lower air masses over the continents. In many cases, however, the forcing parameterizes some indirect physical or dynamical effects that are not explicitly described by the resolved model dynamics. Similar conclusions can be drawn on the role of the empirical linear parameterization. An analysis of the equations, with and without the latter, for most rapidly growing structures in different seasons shows that the full semiempirical model is predicting the expected storm track modes on the winter-hemisphere very well, whereas, this is not the case for the model without empirical linear closure. Thus, it is the empirical linear terms that are effectively controlling the seasonality of storm track dynamics.

Notwithstanding the overwhelming role the empirical part plays in the model, one should keep in mind that the successful incorporation of primitive equation dy-

namics and seasonality into EOF modeling seems to provide a more solid basis than ever before for research concerning low-frequency atmosphere dynamics with the help of low-order models. Further support for this view is provided in a companion paper that analyzes the climate simulated by our reduced models and reconsiders some old questions related to the dimensionality of the climate attractor and the origin of weather regimes.

Acknowledgments. The authors are indebted to R. Haarsma, F. Kwasniok, G. Schmitz, F. Selten, and A. Timmermann for numerous discussions helping us in different phases of the work. Furthermore we would like to acknowledge the helpful comments of C. Penland, K. Fraedrich, and one anonymous reviewer whose comments led to substantial improvements in the manuscript. Special thanks are due to R. Voss for allowing us to use his GCM data. The enormous help of X. Wang in retreiving those data from the archives is also gratefully acknowledged. A major part of the research was done while U.A. was a visiting scientist at KNMI.

APPENDIX

A Gridpoint Model for the Primitive Equations without External Kelvin Waves

The horizontal discretization is done on a staggered Arakawa C grid with longitude and latitude indices i and j, counting eastward from 1 to I_{lon}, and northward from 1 to J_{lat}. For details of the grid specification the reader is refered to Arakawa and Lamb (1981). The vertical grid is also staggered with a corresponding index k counting from 1 to K_{lev}. The distribution of variables is as in Arakawa and Lamb (1977). Our notation differs from there by using half-levels for σ and its time derivative, and full levels for all other fields, instead of even and odd levels. Dynamical quantities are given standard notation, if not specified otherwise. For brevity we introduce the following shortcuts for longitudinal differencing, linear averaging, and arithmetic averaging of some quantity X:

$$(\delta_\lambda X)_{i,\cdot} = X_{i+1/2,\cdot} - X_{i-1/2,\cdot}, \tag{A1}$$

$$(\overline{X}^{\lambda})_{i,\cdot} = \frac{1}{2}(X_{i+1/2,\cdot} + X_{i-1/2,\cdot}), \tag{A2}$$

$$(\widetilde{X^2}^{\lambda})_{i+1/2,\cdot} = X_{i,\cdot}X_{i+1,\cdot}. \tag{A3}$$

Analogous notation holds for the corresponding latitudinal and vertical operations. For the area differential we write $\Delta A = (\Delta\lambda\Delta\phi)/(mn)$. The metric factors are $m = 1/(a\cos\phi)$ and $n = 1/a$. Let us now also define the local product of surface pressure and area differential

$$P^s_{i+1/2,j+1/2} = (\Delta A p^s)_{i+1/2,j+1/2}, \tag{A4}$$

so that shallow water potential vorticity becomes

$$q_{i,j,k} = 4\frac{[\Delta A(f+\zeta)]_{i,j,k}}{P^s_{i+1/2,j+1/2} + P^s_{i-1/2,j+1/2} + P^s_{i+1/2,j-1/2} + P^s_{i-1/2,j-1/2}}, \tag{A5}$$

where relative vorticity is calculated via

$$\zeta_{i,j,k} = \frac{1}{\Delta A_{i,j}}\left(\delta_\lambda\frac{v\Delta\phi}{n} - \delta_\phi\frac{u\Delta\lambda}{m}\right)_{i,j,k}. \tag{A6}$$

Here, ζ and q at the poles are obtained from

$$q_{i,J_{\text{lat}},k} = \frac{(f+\zeta)_{i,J_{\text{lat}},k}}{\left(\sum_{i=1}^{I_{\text{lon}}} p^s_{i,J_{\text{lat}}-1/2}\right)\Big/ I_{\text{lon}}}, \tag{A7}$$

$$q_{i,1,k} = \frac{(f+\zeta)_{i,1,k}}{\left(\sum_{i=1}^{I_{\text{lon}}} p^s_{i,3/2}\right)\Big/ I_{\text{lon}}}, \tag{A8}$$

$$\zeta_{i,J_{\text{lat}},k} = \frac{1}{\Delta A_n}\sum_{i=1}^{I_{\text{lon}}}\left(\frac{u\Delta\lambda}{m}\right)_{i,J_{\text{lat}}-1/2,k}, \quad \text{and} \tag{A9}$$

$$\zeta_{i,1,k} = -\frac{1}{\Delta A_s}\sum_{i=1}^{I_{\text{lon}}}\left(\frac{u\Delta\lambda}{m}\right)_{i,3/2,k}, \tag{A10}$$

with $\Delta A_n = I_{\text{lon}}/2(\Delta A)_{J_{\text{lat}}-1/2}$ and $\Delta A_s = I_{\text{lon}}/2(\Delta A)_{3/2}$.

Furthermore, we introduce the velocity-related quantities

$$u^*_{i,j+1/2,k} = \left(\overline{p^s}^{\lambda}u\frac{\Delta\phi}{n}\right)_{i,j+1/2,k}, \quad \text{and} \tag{A11}$$

$$v^*_{i+1/2,j,k} = \left(\overline{p^s}^{\phi}v\frac{\Delta\lambda}{m}\right)_{i+1/2,j,k}. \tag{A12}$$

With these definitions, the fourth-order accurate analogues of the terms $A^u = -q(vp^s/m)$ and $A^v = q(up^s/n)$ in the momentum equations become (Takano and Wurtele 1982)

$$\begin{aligned} A^u(\mathbf{V}, q)_{i,j+1/2,k} &= -\alpha_{i,j+1/2,k}v^*_{i+1/2,j+1,k} - \beta_{i,j+1/2,k}v^*_{i-1/2,j+1,k} \\ &\quad - \gamma_{i,j+1/2,k}v^*_{i-1/2,j,k} - \delta_{i,j+1/2,k}v^*_{i+1/2,j,k} \\ &\quad + \epsilon_{i+1/2,j+1/2,k}u^*_{i+1,j+1/2,k} - \epsilon_{i-1/2,j+1/2,k}u^*_{i-1,j+1/2,k} \\ &\quad + \lambda_{i,j+1,k}u^*_{i,j+3/2,k} - \lambda_{i,j,k}u^*_{i,j-1/2,k}, \quad \text{and} \end{aligned} \tag{A13}$$

$$A^{v}(\mathbf{V}, q)_{i+1/2,j,k} = \gamma_{i+1,j+1/2,k}u^{*}_{i+1,j+1/2,k} + \delta_{i,j+1/2,k}u^{*}_{i,j+1/2,k} + \alpha_{i,j-1/2,k}u^{*}_{i,j-1/2,k} + \beta_{i+1,j-1/2,k}u^{*}_{i+1,j-1/2,k} + \psi_{i+1/2,j+1/2,k}v^{*}_{i+1/2,j+1,k} - \psi_{i+1/2,j-1/2,k}v^{*}_{i+1/2,j-1,k} + \mu_{i+1,j,k}v^{*}_{i+3/2,j,k} - \mu_{i,j,k}v^{*}_{i-1/2,j,k}. \quad \text{(A14)}$$

Here, the contributing coefficients are

$$\alpha_{i,j+1/2,k} = \frac{1}{24}(2q_{i+1,j+1,k} + 3q_{i,j+1,k} + 2q_{i,j,k} + q_{i+1,j,k} - q_{i,j+2,k} - q_{i-1,j+1,k}),$$

$$\beta_{i,j+1/2,k} = \frac{1}{24}(3q_{i,j+1,k} + 2q_{i-1,j+1,k} + q_{i-1,j,k} + 2q_{i,j,k} - q_{i+1,j+1,k} - q_{i,j+2,k}),$$

$$\gamma_{i,j+1/2,k} = \frac{1}{24}(2q_{i,j+1,k} + q_{i-1,j+1,k} + 2q_{i-1,j,k} + 3q_{i,j,k} - q_{i,j-1,k} - q_{i+1,j,k}),$$

$$\delta_{i,j+1/2,k} = \frac{1}{24}(q_{i+1,j+1,k} + 2q_{i,j+1,k} + 3q_{i,j,k} + 2q_{i+1,j,k} - q_{i-1,j,k} - q_{i,j-1,k}),$$

$$\epsilon_{i+1/2,j+1/2,k} = \frac{1}{24}(q_{i+1,j+1,k} + q_{i,j+1,k} - q_{i,j,k} - q_{i+1,j,k}),$$

$$\psi_{i+1/2,j+1/2,k} = \frac{1}{24}(-q_{i+1,j+1,k} + q_{i,j+1,k} + q_{i,j,k} - q_{i+1,j,k}),$$

$$\lambda_{i,j,k} = \frac{1}{24}(q_{i+1,j,k} - q_{i-1,j,k}), \quad \text{and}$$

$$\mu_{i,j,k} = \frac{1}{24}(q_{i,j-1,k} - q_{i,j+1,k}). \quad \text{(A15)}$$

Finally, one needs kinetic energy at scalar points:

$$K_{i+1/2,j+1/2,k} = \frac{1}{2\Delta A_{i+1/2,j+1/2}}(\overline{\Delta A u^{2}}^{\lambda} + \overline{\Delta A v^{2}}^{\phi})_{i+1/2,j+1/2,k}, \quad \text{(A16)}$$

and the σ velocities above and below horizontal velocity points:

$$\dot{\sigma}^{u}_{i,j+1/2,k+1/2} = \left(\frac{\overline{p^{s}\dot{\sigma}}^{\lambda}}{\overline{p^{s}}^{\lambda}}\frac{\Delta\lambda}{m}\right)_{i,j+1/2,k+1/2}, \quad \text{and} \quad \text{(A17)}$$

$$\dot{\sigma}^{v}_{i+1/2,j,k+1/2} = \left(\frac{\overline{p^{s}\dot{\sigma}}^{\phi}}{\overline{p^{s}}^{\phi}}\frac{\Delta\phi}{n}\right)_{i+1/2,j,k+1/2}. \quad \text{(A18)}$$

The latter enter the vertical momentum advection terms via

$$\left(\dot{\sigma}^{X}\frac{\partial X}{\partial\sigma}\right)_{\cdot,k} = \frac{1}{2\Delta\sigma_{k}}[(X_{\cdot,k+1} - X_{\cdot,k})\dot{\sigma}^{X}_{\cdot,k+1/2} + (X_{\cdot,k} - X_{\cdot,k-1})\dot{\sigma}^{X}_{\cdot,k-1/2}], \quad \text{(A19)}$$

where X is either u or v, and $\Delta\sigma_{k} = \sigma_{k+1/2} - \sigma_{k-1/2}$. With all the definitions given above, the discretized momentum equations are now

$$\left[\frac{\Delta\lambda}{m}\frac{\partial u}{\partial t} + A^{u}(\mathbf{V}, q) + \delta_{\lambda}(K + \Phi) + \sigma\alpha_{v}\delta_{\lambda}p^{s} + \dot{\sigma}^{u}\frac{\partial u}{\partial\sigma}\right]_{i,j+1/2,k} = \left(\frac{F_{\lambda}}{m}\Delta\lambda\right)_{i,j+1/2,k}, \quad \text{and} \quad \text{(A20)}$$

$$\left[\frac{\Delta\phi}{n}\frac{\partial v}{\partial t} + A^{v}(\mathbf{V}, q) + \delta_{\phi}(K + \Phi) + \sigma\alpha_{v}\delta_{\phi}p^{s} + \dot{\sigma}^{v}\frac{\partial v}{\partial\sigma}\right]_{i+1/2,j,k} = \left(\frac{F_{\phi}}{n}\Delta\phi\right)_{i+1/2,j,k}. \quad \text{(A21)}$$

The continuity equation becomes

$$\left(\frac{\partial P^{s}}{\partial t} + \delta_{\lambda}u^{*} + \delta_{\phi}v^{*} + P^{s}\frac{\delta_{\sigma}\dot{\sigma}}{\Delta\sigma}\right)_{i+1/2,j+1/2,k} = 0. \quad \text{(A22)}$$

Discretization of the first law of thermodynamics is done via

$$\left[\frac{\partial}{\partial t}(\tau P^{s}) + \delta_{\lambda}(u^{*}\overline{\tau}^{\lambda}) + \delta_{\phi}(v^{*}\overline{\tau}^{\phi}) + P^{s}\frac{\delta_{\sigma}(\dot{\sigma}\tau)}{\Delta\sigma}\right]_{i+1/2,j+1/2,k} = \left(\frac{P^{s}Q}{2\tau c_{p}P}\right)_{i+1/2,j+1/2,k}, \quad \text{(A23)}$$

with $\tau_{i+1/2,j+1/2,k+1/2} = 1/2(\tau_{i+1/2,j+1/2,k} + \tau_{i+1/2,j+1/2,k+1})$.

Equations (A20) and (A21) need the specific volume at u and v points, given by

$$(\sigma\alpha_{v})_{i,j+1/2,k} = c_{p}\left(\widetilde{\tau^{2}}^{\lambda}\frac{\delta_{\lambda}P}{\delta_{\lambda}p^{s}}\right)_{i,j+1/2,k}, \quad \text{and} \quad \text{(A24)}$$

$$(\sigma\alpha_{v})_{i+1/2,j,k} = c_{p}\left(\widetilde{\tau^{2}}^{\phi}\frac{\delta_{\phi}P}{\delta_{\phi}p^{s}}\right)_{i+1/2,j,k}. \quad \text{(A25)}$$

The hydrostatic equation is solved using

$$\Phi_{i+1/2,j+1/2,k} = \Phi_{i+1/2,j+1/2,k+1} + c_{p}(\widetilde{\tau^{2}}^{\sigma}\delta_{\sigma}P)_{i+1/2,j+1/2,k+1/2}, \quad \text{(A26)}$$

and

$$\Phi_{i+1/2,j+1/2,K_{\rm lev}} = \Phi^s_{i+1/2,j+1/2} + c_p p^s_{i+1/2,j+1/2} \sum_{k=1}^{K_{\rm lev}} \Delta\sigma_k \left(\tau^2 \frac{\partial P}{\partial p^s}\right)_{i+1/2,j+1/2,k} - c_p \sum_{k=1}^{K_{\rm lev}-1} \sigma_{k+1/2} (\widetilde{\tau^2}^{\sigma} \delta_\sigma P)_{i+1/2,j+1/2,k+1/2}. \quad \text{(A27)}$$

What is still lacking is a recipe for calculating P at full levels. With this respect we follow Arakawa and Lamb (1977) by using

$$P_{i+1/2,j+1/2,k} = \left(\frac{p^s_{i+1/2,j+1/2}}{p_0}\right)^{R/c_p} \left(\frac{1}{1+b} \frac{\sigma^{1+b}_{k+1/2} - \sigma^{1+b}_{k-1/2}}{\sigma_{k+1/2} - \sigma_{k-1/2}}\right)^{R/(c_p b)}, \quad \text{(A28)}$$

with $b = 0.205$.

Now, by setting the surface pressure time independent, the continuity equation becomes

$$\left(\delta_\lambda u^* + \delta_\phi v^* + P^s \frac{\delta_\sigma \dot\sigma}{\Delta\sigma}\right)_{i+1/2,j+1/2,k} = 0, \quad \text{(A29)}$$

which yields, after multiplying by $\Delta\sigma_k$ and taking the sum over all levels,

$$(\delta_\lambda \langle u^* \rangle + \delta_\phi \langle v^* \rangle)_{i+1/2,j+1/2,k} = 0, \quad \text{(A30)}$$

where we have used the notation $\langle X \rangle_\cdot = \sum_{k=1}^{K_{\rm lev}} \Delta\sigma_k X_{\cdot,k}$ for the vertical average of an arbitrary quantity X. Equation (A30) implies the existence of a barotropic streamfunction $\Psi_{i,j}$ so that

$$\langle u^* \rangle_{i,j+1/2} = -(\delta_\phi \Psi)_{i,j+1/2}, \quad \text{and} \quad \text{(A31)}$$

$$\langle v^* \rangle_{i+1/2,j} = (\delta_\lambda \Psi)_{i+1/2,j}. \quad \text{(A32)}$$

Given a boundary value of Ψ at one of the poles (we have set $\Psi_{\cdot,J_{\rm lat}} = 0$), it can be determined by first calculating relative barotropic vorticity via

$$\langle \zeta \rangle_{i,j} = \frac{1}{\Delta A_{i,j}} \left(\delta_\lambda \frac{\langle v \rangle \Delta\phi}{n} - \delta_\phi \frac{\langle u \rangle \Delta\lambda}{m}\right)_{i,j}, \quad \text{(A33)}$$

and the corresponding relation for the South Pole, to be obtained from (A10), and then inverting

$$(\Delta A \langle \zeta \rangle)_{i,j} = (\mathbf{V}\Psi)_{i,j}, \quad \text{(A34)}$$

where $\mathbf{V}$ is the vorticity operator, the discretized analogue of $\nabla \cdot (\nabla / p^s)$, whose elements can be obtained from (A33) and its counterpart for the South Pole, (A11), (A12), (A31), and (A32). Finally, let us also introduce the baroclinic velocities $\hat u$ and $\hat v$. For any quantity X we define $\hat X = X - \langle X \rangle$. We now replace u and v as prognostic variables by Ψ and the values of $\hat u$ and $\hat v$ on all levels but the lowest one. Their tendencies can be obtained from $\partial u/\partial t$ and $\partial v/\partial t$ in (A20) and (A21), by calculating first the time derivative of relative barotropic vorticity from

$$\left(\frac{\partial \langle \zeta \rangle}{\partial t}\right)_{i,j} = \frac{1}{\Delta A_{i,j}} \left(\delta_\lambda \frac{\left\langle \frac{\partial v}{\partial t} \right\rangle \Delta\phi}{n} - \delta_\phi \frac{\left\langle \frac{\partial u}{\partial t} \right\rangle \Delta\lambda}{m}\right)_{i,j}, \quad \text{(A35)}$$

and the corresponding relation at the South Pole,

$$\left(\frac{\partial \langle \zeta \rangle}{\partial t}\right)_{i,1} = -\frac{1}{\Delta A_s} \sum_{i=1}^{I_{\rm lon}} \left(\frac{\left\langle \frac{\partial u}{\partial t} \right\rangle \Delta\lambda}{m}\right)_{i,3/2}, \quad \text{(A36)}$$

and then determining the barotropic streamfunction tendencies from the time derivative of (A34). Additionally,

$$\left(\frac{\partial \hat u}{\partial t}\right)_{i,j+1/2,k} = \left(\frac{\partial u}{\partial t} - \left\langle \frac{\partial u}{\partial t} \right\rangle\right)_{i,j+1/2,k}, \quad \text{and} \quad \text{(A37)}$$

$$\left(\frac{\partial \hat v}{\partial t}\right)_{i+1/2,j,k} = \left(\frac{\partial v}{\partial t} - \left\langle \frac{\partial v}{\partial t} \right\rangle\right)_{i+1/2,j,k}, \quad \text{(A38)}$$

yield the tendencies of the baroclinic velocities. It should be mentioned that the surface geopotential height does not appear in the final dynamic equations. The orographic impact is mediated indirectly to the model by the surface pressure distribution that mirrors the surface height variations over the globe. Using some algebra one can check that the continuous model actually conserves total energy E_f as given in (14), and that the discretized equations conserve its analogue $E_f = E^{\rm kin}_{\rm btp} + E^{\rm kin}_{\rm bcl} + E^{\rm th}$ (defining the total energy norm), where the barotropic and baroclinic parts of kinetic energy are, respectively,

$$E^{\rm kin}_{\rm btp} = \frac{1}{g} \sum_{i=1}^{I_{\rm lon}} \left\{ \sum_{j=2}^{J_{\rm lat}-1} \left[\frac{m\Delta\phi}{n\Delta\lambda} \frac{(\delta_\lambda \Psi)^2}{2\overline{p^s}^{\phi}}\right]_{i+1/2,j} + \sum_{j=1}^{J_{\rm lat}-1} \left[\frac{n\Delta\lambda}{m\Delta\phi} \frac{(\delta_\phi \Psi)^2}{2\overline{p^s}^{\lambda}}\right]_{i,j+1/2} \right\}, \quad \text{and} \quad \text{(A39)}$$

$$E^{\rm kin}_{\rm bcl} = \frac{1}{g} \sum_{i=1}^{I_{\rm lon}} \sum_{k=1}^{K_{\rm lev}} \Delta\sigma_k \left[\sum_{j=1}^{J_{\rm lat}-1} \left(\Delta A \overline{p^s}^{\lambda} \frac{\hat u^2}{2}\right)_{i,j+1/2,k} + \sum_{j=2}^{J_{\rm lat}-1} \left(\Delta A \overline{p^s}^{\phi} \frac{\hat v^2}{2}\right)_{i+1/2,j,k} \right], \quad \text{(A40)}$$

and total enthalpy is given by

$$E^{\rm th} = \frac{1}{g} \sum_{i=1}^{I_{\rm lon}} \sum_{j=1}^{J_{\rm lat}-1} \sum_{k=1}^{K_{\rm lev}} \Delta\sigma_k c_p (P^s P \tau^2)_{i+1/2,j+1/2,k}. \quad \text{(A41)}$$

More details can be found online at http:/www.iap-kborn.de/mitarbeiter/index_e.htm.

REFERENCES

Achatz, U., and G. Schmitz, 1997: On the closure problem in the reduction of complex atmospheric models by PIPs and EOFs: A comparison for the case of a two-layer model with zonally symmetric forcing. *J. Atmos. Sci.*, **54,** 2452–2474.

——, and G. Branstator, 1999: A two-layer model with empirical linear corrections and reduced order for studies of internal climate variability. *J. Atmos. Sci.,* **56,** 3140–3160.
Arakawa, A., and V. R. Lamb, 1977: Computational design of the basic dynamical processes of the UCLA general circulation model. *Methods Comput. Phys.,* **17,** 173–265.
——, and ——, 1981: A potential enstrophy and energy conserving scheme for the shallow water equations. *Mon. Wea. Rev.,* **109,** 18–36.
Asselin, R., 1972: Frequency filter for time integrations. *Mon. Wea. Rev.,* **100,** 487–490.
Bryan, K., 1969: A numerical method for the study of the circulation of the World Ocean. *J. Comput. Phys.,* **4,** 347–376.
Charney, J., and J. G. DeVore, 1979: Multiple flow equilibria in the atmosphere and blocking. *J. Atmos. Sci.,* **36,** 1205–1216.
Corti, S., F. Molteni, and T. N. Palmer, 1999: Signature of recent climate change in frequencies of natural atmospheric circulation regimes. *Nature,* **398,** 799–802.
d'Andrea, F., and R. Vautard, 2001: Extratropical low-frequency variability as a low-dimensional problem. I: A simplified model. *Quart. J. Roy. Meteor. Soc.,* **127,** 1357–1374.
DelSole, T., 2001: A theory for the forcing and dissipation in stochastic turbulence models. *J. Atmos. Sci.,* **58,** 3762–3775.
——, and A. Y. Hou, 1999: Empirical stochastic models for the dominant climate statistics of a general circulation model. *J. Atmos. Sci.,* **56,** 3436–3456.
Farrell, B. F., and P. J. Ioannou, 1993: Stochastic dynamics of baroclinic waves. *J. Atmos. Sci.,* **50,** 4044–4057.
——, and ——, 1994: A theory for the statistical equilibrium energy spectrum and heat flux produced by transient baroclinic waves. *J. Atmos. Sci.,* **51,** 2685–2698.
——, and ——, 1996: Generalized stability theory. Part I: Autonomous operators. *J. Atmos. Sci.,* **53,** 2025–2040.
Hannachi, A., 1997: Low-frequency variability in a GCM: Three-dimensional flow regimes and their dynamics. *J. Climate,* **10,** 1357–1379.
Held, I. M., and M. J. Suarez, 1978: A two-level primitive equation atmospheric model designed for climate sensitivity experiments. *J. Atmos. Sci.,* **35,** 206–229.
——, and ——, 1994: A proposal for the intercomparison of the dynamical cores of atmospheric general circulation models. *Bull. Amer. Meteor. Soc.,* **75,** 1825–1830.
Legras, B., and M. Ghil, 1985: Persistent anomalies, blocking and variations in atmospheric predictability. *J. Atmos. Sci.,* **42,** 433–471.
Lorenz, E. N., 1963: Deterministic nonperiodic flow. *J. Atmos. Sci.,* **20,** 130–141.
Michelangeli, P.-A., R. Vautard, and B. Legras, 1995: Weather regimes: Recurrence and quasi stationarity. *J. Atmos. Sci.,* **52,** 1237–1256.
Moise, I., and R. Temam, 2000: Renormalization group method: Application to Navier–Stokes equation. *Discrete Contin. Dyn. Syst.,* **6,** 191–210.
Penland, C., and L. Matrosova, 1994: A balance condition for stochastic numerical models with application to the El Niño–Southern Oscillation. *J. Climate,* **7,** 1352–1372.
——, and P. D. Sardeshmukh, 1995: The optimal growth of tropical sea surface temperature anomalies. *J. Climate,* **8,** 1999–2024.
Phillips, N. A., 1959: An example of nonlinear computational instability. *The Atmosphere and Sea in Motion: Rossby Memorial Volume,* B. Bolin, Ed., Rockefeller Institute Press, 501–504.
Rinne, J., and V. Karhilla, 1975: A spectral barotropic model in horizontal empirical orthogonal functions. *Quart. J. Roy. Meteor. Soc.,* **101,** 365–382.
Selten, F. M., 1995: An efficient description of the dynamics of barotropic flow. *J. Atmos. Sci.,* **52,** 915–936.
——, 1997a: A statistical closure of a low-order barotropic model. *J. Atmos. Sci.,* **54,** 1085–1093.
——, 1997b: Baroclinic empirical orthogonal functions as basis functions in an atmospheric model. *J. Atmos. Sci.,* **54,** 2099–2114.
Smagorinsky, J., 1963: General circulation experiments with the primitive equations. I. The basic experiment. *Mon. Wea. Rev.,* **91,** 99–164.
Takano, K., and M. G. Wurtele, 1982: A fourth-order energy and potential enstrophy conserving difference scheme. AFGL Tech. Rep. 82-0205, Air Force Geophysics Laboratory, 85 pp.
Vautard, R., and B. Legras, 1988: On the source of midlatitude low-frequency variability. Part II: Nonlinear equilibration of weather regimes. *J. Atmos. Sci.,* **45,** 2845–2867.
Voss, R., R. Saussen, and U. Cubasch, 1998: Periodically synchronously coupled integrations with the atmosphere–ocean general circulation model ECHAM3/LSG. *Climate Dyn.,* **14,** 249–266.
Whitaker, J. S., and P. D. Sardeshmukh, 1998: A linear theory of extratropical synoptic eddy statistics. *J. Atmos. Sci.,* **55,** 237–258.
Zhang, Y., and I. M. Held, 1999: A linear stochastic model of a GCM's midlatitude storm tracks. *J. Atmos. Sci.,* **56,** 3416–3435.